Am J Cancer Res 2016;6(2):473-485
www.ajcr.us /ISSN:2156-6976/ajcr0022517

Original Article

PFKL/miR-128 axis regulates glycolysis by inhibiting AKT phosphorylation and predicts poor survival in lung cancer

Jie Yang[1,2], Jingqiu Li[1,2], Yanping Le[1,2], Chengwei Zhou[3], Shun Zhang[4], Zhaohui Gong[1,2]

[1]Department of Biochemistry and Molecular Biology, Ningbo University School of Medicine, Ningbo, ZJ 315211, China; [2]Zhejiang Provincial Key Laboratory of Pathophysiology, Ningbo University School of Medicine, Ningbo, ZJ 315211, China; [3]Department of Chest Surgery, The Affiliated Hospital of Ningbo University School of Medicine, Ningbo, ZJ 315020, China; [4]Clinical Laboratory, Ningbo No. 2 Hospital, Ningbo, ZJ 315010, China

Received December 22, 2015; Accepted January 3, 2016; Epub January 15, 2016; Published February 1, 2016

Abstract: MicroRNAs (miRNAs) affect cancer cell glucose metabolism by targeting mRNAs of diverse enzymes that have been implicated in oxidative phosphorylation (OXPHOS) and glycolytic pathways. However, the mechanisms that underlie miRNA-mediated regulation of phosphofructokinase (*PFK*), a key rate-limiting enzyme in glycolysis, remain largely unknown. Here, we show that miR-128 directly targets *PFK* liver type (*PFKL*) in lung cancer cells and regulates endogenous expression of *PFKL* at both the mRNA and protein levels. In line with this, overexpression of miR-128 decreased glucose uptake and lactate production, as well as increased cellular ATP content. Interestingly, knockdown of miR-128 was shown to promote lung cancer cell growth and colony formation. Moreover, we observed that miR-128 expression inversely correlated with *PFKL* mRNA levels in clinic lung cancer samples and that increased *PFKL* expression predicted poor overall survival in lung cancer patients. Mechanistically, we showed that miR-128 regulates *PFKL* via a feedback loop that involves inhibition of the AKT signaling pathway. Together, our results suggest that miR-128 acts as a metabolic regulator in lung cancer cells that may be therapeutically exploited.

Keywords: microRNA, phosphofructokinase, glycolysis, phosphorylation, lung cancer

Introduction

The shift from oxidative phosphorylation (OXPHOS) to glycolysis is a hallmark of cancer cells. In contrast to normal cells, cancer cells preferentially metabolize glucose into lactate for energy production, despite the presence of abundant oxygen [1, 2]. This metabolic change is critical for cancer cell proliferation, migration and metastasis [3]. Accumulating evidences suggest that targeting enzymes involved in the glycolytic pathway may open a therapeutic window to modulate cancer cell glucose metabolism and suppress cancer progression [4]. In particular, suppression of lactate dehydrogenase A (LDH-A) has been shown to inhibit cell growth and enhance the levels of OXPHOS in multiple tumor cells [5]. Moreover, *Pten-/p53*-deficiency-driven tumor growth *in vivo* has been shown to depend on hexokinase 2 (HK2), an enzyme that catalyzes the first irreversible step of glycolysis and mediates aerobic glycolysis [6]. Together, these studies directly link the metabolic enzymes that regulate aerobic with tumorigenesis.

Phosphofructokinase (PFK) is a key rate-limiting enzyme that catalyzes the phosphorylation of fructose-6-phosphate to fructose-1,6-bisphosphate, which is a critical regulatory step during the glycolytic pathway [7]. Interestingly, recent studies indicate that glycosylation of PFK1 at Ser529 promotes the shift from glycolysis to pentose phosphate pathway and therefore protect cells from death. Moreover, suppression of PFK1 expression inhibited cell proliferation and tumorigenicity [8]. The *PFKFB2* gene is a *PFK* isoform that is a direct target of the androgen receptor and has been shown to participate in glucose-dependent lipid synthesis and modulate glucose uptake via PI3K/AKT signaling in prostate cancer [9]. These observations indi-

cate that PFK is deeply involved in glucose metabolism. However, the mechanisms that underlie epigenetic regulation of PFK expression and how PFK regulates glycolysis remain poorly understood.

MicroRNAs (miRNAs) are a class of endogenous, small non-coding RNAs that function at the post-transcriptional level by targeting 3'untranslated regions (3'UTR) of mRNAs [10, 11]. Many studies have linked miRNAs to basic biological processes, such as cell proliferation [12], glucose metabolism [13], differentiation and apoptosis [14]. In addition, our previous studies have implicated deregulated miRNA expression in lung cancer cell cycle modulation [15], drug resistance [16] and tumor metastasis [17]. Recently, miRNAs have been reported to regulate glucose metabolism by modulating the expression of glycolytic pathway [3]. For example, the tumor suppressive function of miR-143 [18] has linked to its ability to down-regulate the glucose uptake and lactate production by inhibiting HK2 activity in CRL-5803 cells [19]. In contrast, miR-378* increased lactate levels, reduced oxygen consumption and tricarboxylic acid (TCA) cycle-associated gene expression, and drove a metabolic shift from OXPHOS to glycolysis in breast cancer cells [13]. miR-155 has also been shown to act as an oncogenic miRNA by up-regulating HK2 expression and driving glycolysis through activation of STAT3 in breast cancer cells [20]. These results indicate that miRNAs may regulate glycolysis and TCA pathways by targeting key enzymes involved in glucose metabolism. However, whether miRNAs play a role in regulating PFK-driven glycolysis in cancer cells glycolysis is largely unknown. In this study, we report that miR-128 regulates PFKL (PFK liver type) expression and mediates a shift from glycolysis to OXPHOS in lung cancer cells by modulating AKT phosphorylation.

Materials and methods

Cell culture and reagents

Lung cancer cell lines (SPC-A-1, LTEP-a-2, A549, NCI-H460 and NCI-H1299), normal lung epithelial cell line (BEAS-2B) and human embryonic kidney cell line (293T) were purchased from Chinese Academy of Sciences Cell Bank of Type Culture Collection (CBTCCCAS). SPC-A-1 and LTEP-a-2 cell lines were cultured in RPMI-1640 (Invitrogen, USA) medium supplemented with 10% FBS (ExCell Bio, China) and 2.5 g/L glucose, 0.11 g/L sodium pyruvate. A549, NCI-H460, NCI-H1299 and BEAS-2B cell lines were cultured in RPMI-1640 medium with 10% FBS only. 293T cells were cultured in Dulbecco's modified Eagle's medium (DMEM; Invitrogen, USA) supplemented with 10% FBS only. All of these cells were maintained in 5% CO_2 at 37°C. The AKT inhibitor GSK690693 was purchased from Selleck Chemicals (Selleck, USA).

siRNA experiments

Cells were transfected with Lipofectamine 2000 (Invitrogen, USA) according to the manufacturer's protocol with 50 nM PFKL and AKT siRNA (or the corresponding control siRNA). Cells were harvested 24 hours post-transfection with si-PFKL and si-AKT to achieve maximal knockdown.

RNA extraction, reverse transcription, and quantitative real-time PCR

RNA was extracted from cells using RNAiso Plus (TAKARA, Japan) including RNase treatment. To quantitate miR-128 levels, the Hairpin-it™ miR qPCR quantification kit (GenePharma, China) was used, and the corresponding qRT-PCR reactions were carried out on an Mx3005P system (Stratagene, USA). Reactions were performed in an 8-strip tube (Axygen, USA) under the following cycling conditions: 95°C for 3 min, 40 cycles of 95°C for 12 s, 62°C for 40 s. The small nuclear RNA U6 was used to normalize the expression of miR-128. To quantitate *PFKL* and *AKT* mRNA levels, reactions were performed in an 8-strip tube under the following cycling conditions: 95°C for 3 min, 40 cycles of 95°C for 15 s, 53°C for 30 s, and 72°C for 1 min, and a final extension at 72°C for 3 min. Housekeeping gene *β-actin* was used to normalize the expression of *PFKL* and *AKT*.

miRNA mimics and miRNA inhibitor transfection

Twenty-four hours post seeding, cells were transfected using Lipofectamine 2000 with miRNA mimics or inhibitor (or the corresponding control mimics and inhibitor) (GenePharma, China) and cells were harvested 24 hours or 48 hours post-transfection for qRT-PCR or western blot experiment, respectively. Sequences of RNAi are shown in Table S1.

Plasmid construction and dual-luciferase reporter assays

To construct the *PFKL* 3'UTR reporter plasmid, wild-type (WT) or mutated (Mut) sequences of the human *PFKL* 3'UTR that were predicted to be targeted by miR-128 were cloned into the linearized pGL3-control vector (Biogle Biotechnology, China). To construct the *PFKL* overexpression plasmid, the open reading frame of *PFKL* was cloned into the linearized pcDNA3 vector (Biogle Biotechnology, China). The primers used for the construction of pcDNA-PFKL are shown in Table S2. 293T cells were seeded in 6-well plates (1×10^5 cells/well) and incubated for 24 h prior to transfection. For the dual-luciferase assay, cells were co-transfected with 1 μg of pGL3-PFKL-3'UTR or pGL3-PFKL-3'UTR Mut plasmid, 0.5 μg of the pRL-SV40 control vector (Promega, USA). Firefly and Renilla luciferase activities were measured consecutively using a dual luciferase assay kit (Promega, USA) 24 h after transfection.

Western blot analysis

Forty-eight hours post-transfection of miR-128 mimics or inhibitor, proteins were isolated with lysates buffer after washed three times with 1 × PBS, and then quantified using the Bradford procedure (Bio-Rad, USA). Approximately 50 μg of total protein were loaded onto a 12% SDS-PAGE gel and subsequently transferred onto a nitrocellulose transfer membrane (Whatman, Germany). Membranes were incubated in blocking buffer (Li-COR, USA) for 1 hour at room temperature and then incubated with the primary antibodies (anti-PFKL 1:1000; anti-AKT 1:1000; anti-pAKT (CST, USA) 1:2000; anti-GAPDH (Santa Cruz, USA) 1:500) overnight at 4°C. A fluorescent goat anti-rabbit (Li-COR, USA) secondary antibody was used at a dilution of 1:15,000 and protein bands were detected using the infrared imaging system (Li-COR, USA). The level of GAPDH was used to semi-quantitatively analyze the protein levels.

Glucose uptake, lactate production and ATP content assays

Cells were seeded into 96-well plates and transfected with RNAs or pcDNA-PFKL. Twenty-four hours post-transfection, glucose uptake was measured according to the manufacturer's instructions (BioVision, USA). To measure lactate production, cells were seeded into 6-well plates and 24 hours post-tranfection with RNAs or pcDNA-PFKL, lactate production was assessed using a Lactate Colorimetric Assay Kit (BioVision, USA). To detect cellular ATP content, cells were seeded into 6-well plates and transfected with RNAs or pcDNA-PFKL. Intracellular ATP content was then measured 24 hours post-transfection according to the manufacturer's protocol (Beyotime, China).

Cell viability assay

A total of 5×10^3 cells were seeded into 96-well plates and grown for 24, 48, 72 hour post-transfection. Twenty microliters of 5 mg/ml MTT was then added to each well and incubated in 5% CO_2 at 37°C for 4 hours. Following incubation, the media was carefully removed and 150 μl of DMSO was added to each well to dissolve the formazan produced from MTT by the viable cells. Absorbance at 490 nm was read using an automatic microplate reader (Labsystems, Finland).

Colony formation assay

Following genetic or chemical perturbation, NCI-H460 and NCI-H1299 cells were collected as a single cells suspension in medium and 500 cells were seeded into 6-well plates and cultured in 5% CO_2 at 37°C for 10d, with media replaced on the fifth day. Colonies were washed with 1×PBS for three times, fixed with 4% paraformaldehyde for 5 min and stained for 30 s with 0.1% crystal violet. The colony formation assay was repeated in three independent experiments with duplicate wells.

Specimen collection

Tumor tissue and matching normal tissue were collected from 20 patients who underwent surgical resection of lung cancer at the Affiliated Hospital of Ningbo University School of Medicine. For all collected samples, patients had not received prior adjuvant chemotherapy. This study was approved by the Medical Ethical Committee at Ningbo University, and all participants were given written informed consent.

Kaplan-Meier analysis

The relationship between *PFKL* mRNA level and lung cancer patient was analyzed using 1926 lung samples that are available on the public

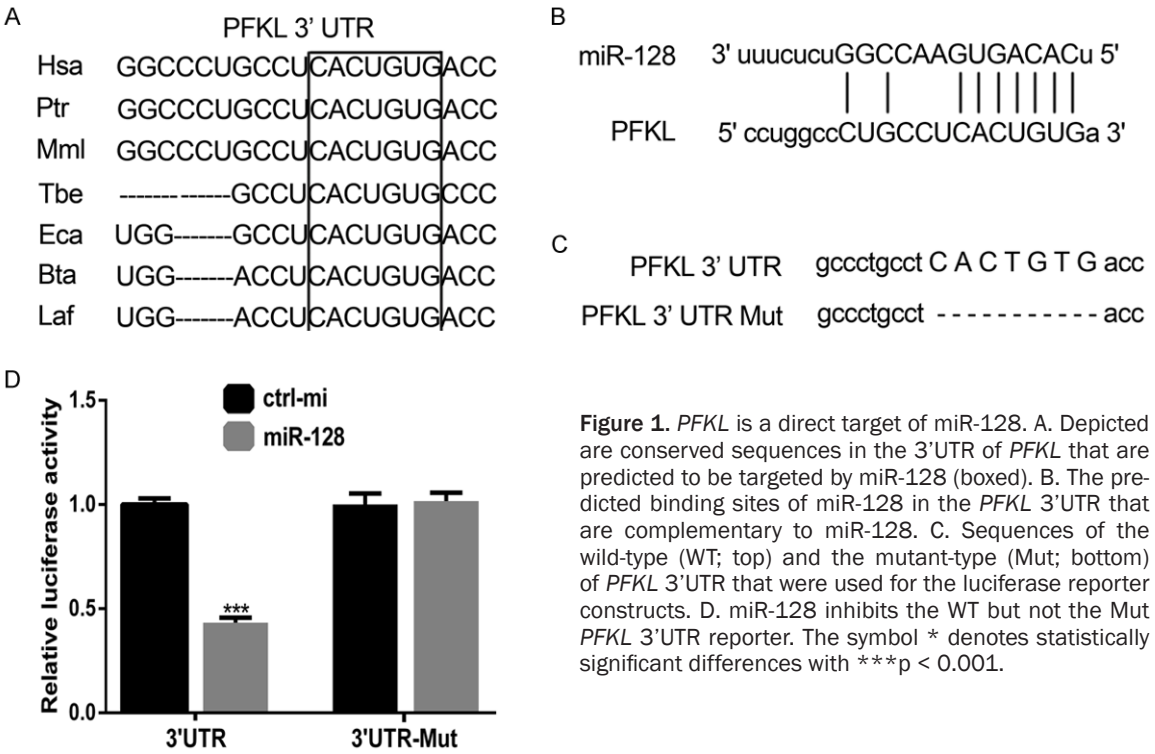

Figure 1. *PFKL* is a direct target of miR-128. A. Depicted are conserved sequences in the 3'UTR of *PFKL* that are predicted to be targeted by miR-128 (boxed). B. The predicted binding sites of miR-128 in the *PFKL* 3'UTR that are complementary to miR-128. C. Sequences of the wild-type (WT; top) and the mutant-type (Mut; bottom) of *PFKL* 3'UTR that were used for the luciferase reporter constructs. D. miR-128 inhibits the WT but not the Mut *PFKL* 3'UTR reporter. The symbol * denotes statistically significant differences with ***$p < 0.001$.

databases (KM plotter, 2015 version, http://kmplot.com/analysis/index.php?p=service&cancer=lung) [4].

Statistical analysis

Statistical analyses were assessed using GraphPad Prism Software 6.0 (GraphPad, USA). All of the experiments were repeated in triplicate and the experimental data were expressed as the mean ± SD. For comparison analysis, Student's *t* test was used. The *p* value < 0.05 was considered statistically significant.

Results

PFKL 3'UTR is a direct target of miR-128

To search for potential candidate miRNAs that target *PFKL*, the following computer-based databases were searched: TargetScan 6.2 (http://www.targetscan.org), microRNA.org (http://www.microrna.org/) and PicTar (http://pictar.mdc-berlin.de/). *PFKL* 3'UTR was conserved among species (**Figure 1A**) and was predicted to be specifically complementary with miR-128 (**Figure 1B**). To validate whether *PFKL* 3'UTR is the direct target of miR-128, the wild type (WT) or mutant type (Mut) sequences of *PFKL* 3'UTR (**Figure 1C**) were cloned downstream of the firefly luciferase reporter gene (pGL3-control). The WT or Mut reporter plasmids were co-transfected with miR-128 mimics (miR-128), control mimics (ctrl-mi) or the control plasmid (pRL-SV40), and then a dual luciferase reporter assay was performed. A marked decrease in luciferase activity was detected when the miR-128 was co-transfected with the WT and the control plasmid (**Figure 1D**, left, $p < 0.001$). In contrast, no visible difference in luciferase activity was observed between ctrl-mi and miR-128 that was co-transfected with the Mut and the control plasmid (**Figure 1D**, right). These results indicate that miR-128 directly targets the 3'UTR of *PFKL*.

MiR-128 negatively regulates PFKL expression in lung cancer cells

To screen for proper cell lines to use in subsequent experiments, we first tested the basal expression of miR-128 and *PFKL* in five lung cancer cell lines and in the normal lung epithelial cell, BEAS-2B. We found that *PFKL* mRNA was highly expressed in NCI-H460 cells and miR-128 was highly expressed in NCI-H1299

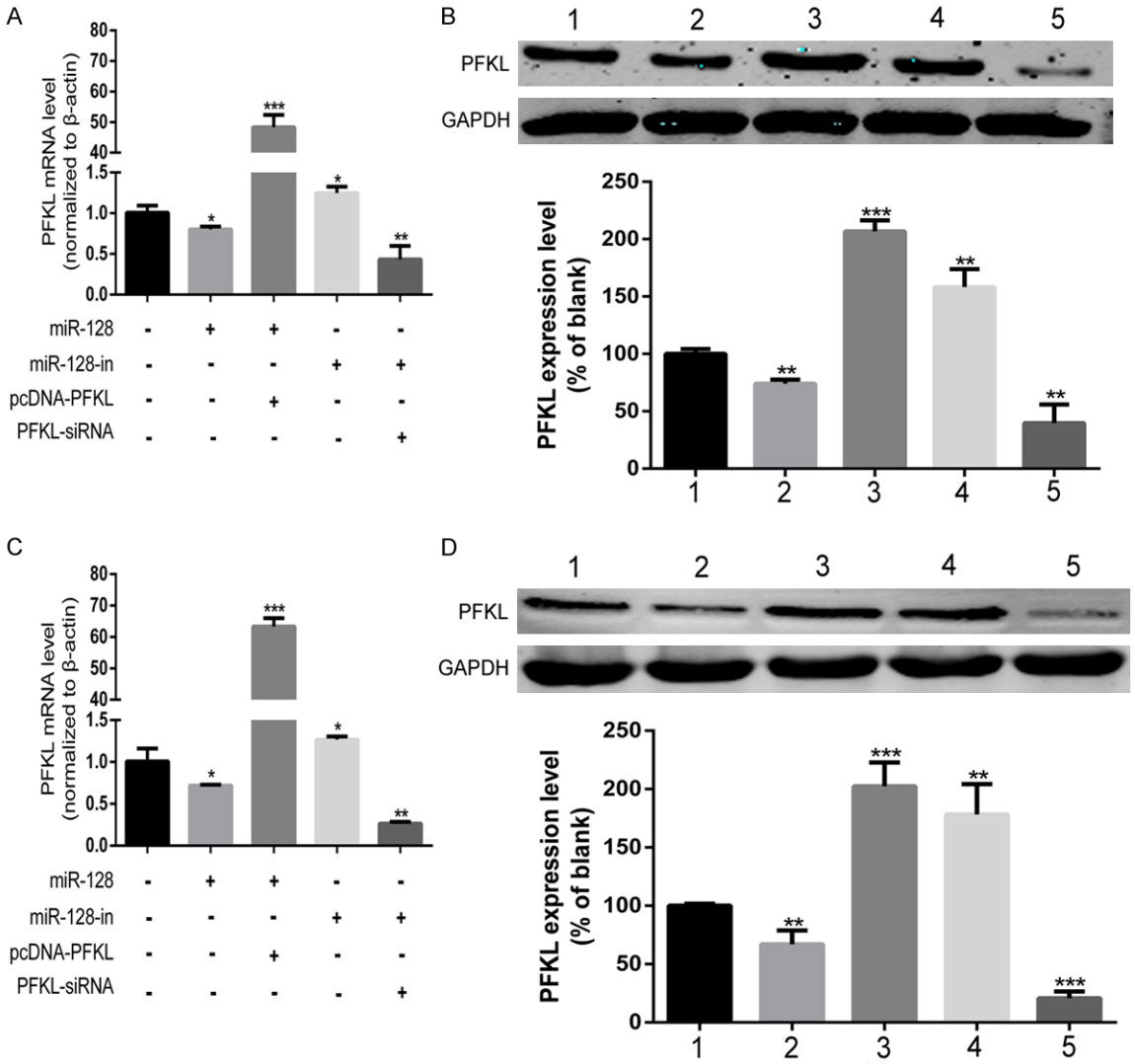

Figure 2. miR-128 targets endogenous *PFKL* and downregulates its expression in lung cancer cells. A and C. Exogenous overexpression of *PFKL* prevents miR-128-mediated repression of *PFKL* mRNA levels in NCI-H460 and NCI-H1299 cells, respectively. *PFKL* mRNA level was measured by qRT-PCR and β-actin was used as a control. B and D. Exogenous overexpression of *PFKL* prevents miR-128-mediated repression of PFKL protein expression in NCI-H460 and NCI-H1299 cells, respectively. PFKL protein expression was measured by western blot and GAPDH was used as a loading control. Lane 1-5: blank, miR-128, miR-128+pcDNA-PFKL, miR-128-in and miR-128-in+PFKL-siRNA. The symbol * shows statistically significant differences with *$p < 0.05$, **$p < 0.01$ and ***$p < 0.001$.

cells compared to normal cells (Figure S1A, S1B). Based on the above evidence that *PFKL* is a direct target of miR-128, we further investigated whether miR-128 regulates endogenous *PFKL* expression in NCI-H460 and NCI-H1299 cells. Using qRT-PCR and western blot analyses, we showed that miR-128 overexpression in NCI-H460 and NCI-H1299 cells significantly decreased *PFKL* expression at mRNA and protein levels compared to control treatments ($p < 0.01$, **Figure 2A-D**, and Figure S2A, S2B). In addition, downregulation of miR-128 via treatment with a miR-128 inhibitor (miR-128-in) in both NCI-H460 and NCI-H1299 cells led to a significant increase of endogenous *PFKL* mRNA and protein levels ($p < 0.01$; **Figure 2A-D**, and Figure S2C, S2D). Together, these results indicate that miR-128 negatively regulates PFKL expression in lung cancer cells.

To characterize the effects of PFKL on mature miR-128 expression, siRNA-mediated knockdown was used to inhibit *PFKL* mRNA and protein levels in NCI-H460 and NCI-H1299 cells

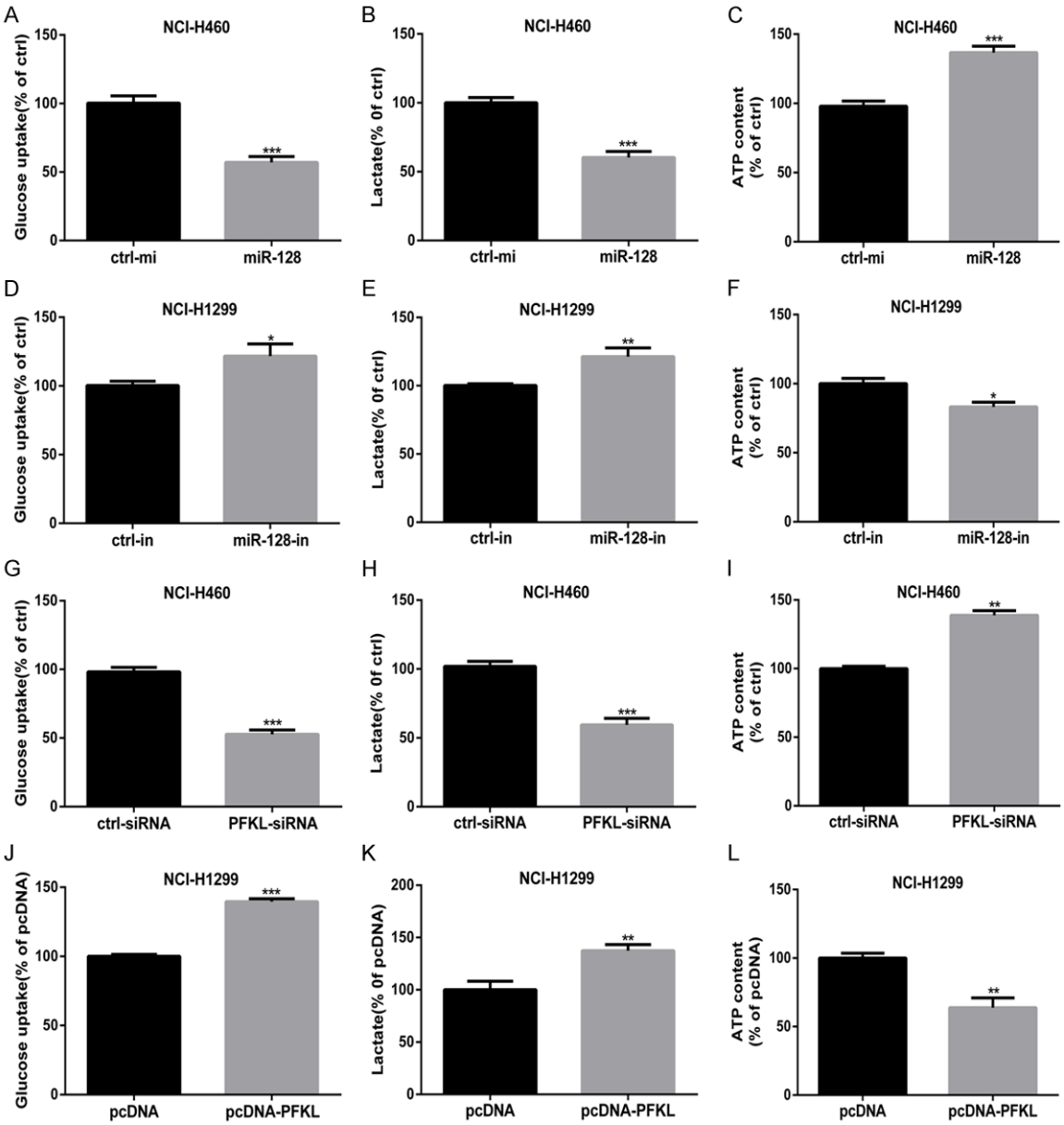

Figure 3. miR-128 induces a metabolic alteration shift in lung cancer cells. A. A decrease in glucose uptake post-transfection with miR-128 mimics in NCI-H460 cells. B. A decrease in lactate production post-transfection with miR-128 mimics in NCI-H460 cells. C. An increase in cellular ATP content post-transfection with miR-128 mimics in NCI-H460 cells. D. An increase in glucose uptake post-transfection with miR-128 inhibitor in NCI-H1299 cells. E. An increase in lactate production post-transfection with miR-128 inhibitor in NCI-H1299 cells F. A decrease in cellular ATP content post-transfection with miR-128 inhibitor in NCI-H1299 cells. G. A decrease in glucose uptake post-transfection with *PFKL* siRNA in NCI-H460 cells. H. A decrease in lactate production post-transfection with *PFKL* siRNA in NCI-H460 cells. I. An increase in cellular ATP content post-transfection with *PFKL* siRNA in NCI-H460 cells. J. An increase in glucose uptake post-transfection with pcDNA-PFKL in NCI-H1299 cells. K. An increase in lactate production post-transfection with pcDNA-PFKL in NCI-H1299 cells. L. A decrease in cellular ATP content post-transfection with pcDNA-PFKL in NCI-H1299 cells. The symbol * denotes statistically significant differences with *$p < 0.05$, **$p < 0.01$ and ***$p < 0.001$.

compared to the control siRNA (ctrl-siRNA) ($p < 0.001$; Figure S2E, S2F). Moreover, PFKL overexpression could notably increase *PFKL* expression both on mRNA ($p < 0.05$) and protein ($p < 0.001$) levels compared to the empty vector (pcDNA) (Figure S2G, S2H). Strikingly, the suppression of *PFKL* mRNA and protein level caused by miR-128 were rescued when

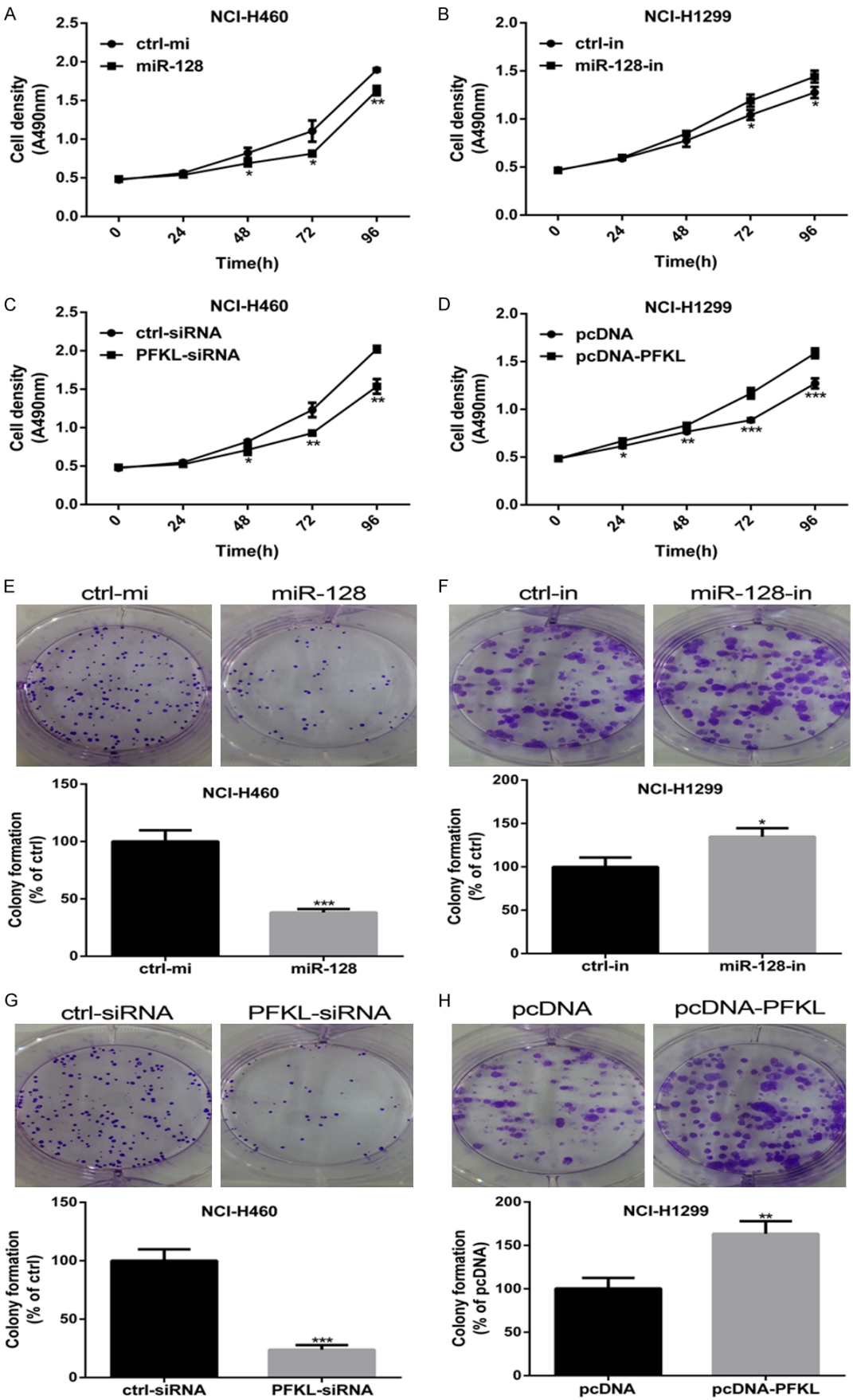
A
NCI-H460
ctrl-mi
miR-128
Cell density (A490nm)
Time(h)
B
NCI-H1299
ctrl-in
miR-128-in
Cell density (A490nm)
Time(h)
C
NCI-H460
ctrl-siRNA
PFKL-siRNA
Cell density (A490nm)
Time(h)
D
NCI-H1299
pcDNA
pcDNA-PFKL
Cell density (A490nm)
Time(h)
E
ctrl-mi
miR-128
NCI-H460
Colony formation (% of ctrl)
F
ctrl-in
miR-128-in
NCI-H1299
Colony formation (% of ctrl)
G
ctrl-siRNA
PFKL-siRNA
NCI-H460
Colony formation (% of ctrl)
H
pcDNA
pcDNA-PFKL
NCI-H1299
Colony formation (% of pcDNA)

Figure 4. Overexpression of miR-128 or downregulation of *PFKL* inhibits lung cancer cell growth and colony formation *in vitro*. A-D. NCI-H460 cells were treated with miR-128 mimics or *PFKL* siRNA, and NCI-H1299 cells were treated with miR-128 inhibitors or pcDNA-PFKL, and MTT assay was performed to measure the cell growth at 24, 48, 72 and 96 h post-transfection. E-H. Representative results of colony formation capacity in lung cancer cells. Cells were treated as described above. The symbol * shows statistically significant differences with *$p < 0.05$, **$p < 0.01$ and ***$p < 0.001$.

pcDNA-PFKL was co-transfected with miR-128 (**Figure 2A-D**). Taken together, the data demonstrate that miR-128 negatively regulates endogenous *PFKL* expression by targeting its 3'UTR.

MiR-128 induces a metabolic shift from glycolysis to OXPHOS in lung cancer cells

Considering the critical role of *PFKL* in cancer glucose metabolism, we assessed whether miR-128 induced change in glucose consumption and drove a shift in energy metabolic programming from glycolysis to OXPHOS in cancer cells. In line with this, transfection of miR-128 mimics and *PFKL* siRNA in NCI-H460 cells led to an upregulation of miR-128 expression and decreased glucose uptake (**Figure 3A**), and lactate production (**Figure 3B**), as well as concomitant and increase in cellular ATP content (**Figure 3C**). Consistent with this, *PFKL* knockdown by siRNA also significantly decreased glucose uptake (**Figure 3G**) and lactate production (**Figure 3H**), and increased cellular ATP content (**Figure 3I**). In contrast, miR-128 overexpression led to an increase in glucose uptake (**Figure 3D**) and lactate production (**Figure 3E**), and a reduction in cellular ATP content (**Figure 3F**) in NCI-H1299 cells. Similarly, *PFKL* overexpression induced an increase in glucose uptake (**Figure 3J**) and lactate production (**Figure 3K**), and reduced cellular ATP content (**Figure 3L**) in NCI-H1299 cells. Together, these gain-of-function and loss-of-function experiments demonstrate that miR-128 regulates the glucose metabolism in human lung cancer cells. Specifically, our data suggests that miR-128 may mediate a metabolic shift from glycolysis to OXPHOS.

MiR-128 modulates cancer cell growth and colony formation by regulating PFKL expression

To elucidate the effect of miR-128 on lung cancer cell growth and proliferation, the 3-(4, 5-dimethylthiazol-2-yl)-2,5-diphenyltetrazolium bromide (MTT) and colony formation assays were performed. As shown in **Figure 4A**, miR-128 overexpression markedly suppressed NCI-H460 cell growth, and colony formation capacity (**Figure 4E**). On the contrary, miR-128 knockdown promoted cancer cell growth (**Figure 4B**) and colony formation (**Figure 4F**). Moreover, siRNA-mediated knockdown of *PFKL* inhibited cancer cell growth (**Figure 4C**) and colony formation (**Figure 4G**). In line with these results, overexpression of *PFKL* in NCI-H1299 cells promoted cancer cell growth (**Figure 4D**) and colony formation (**Figure 4H**). These results indicate that ectopic expression of miR-128 and PFKL are involved in cancer cell growth and colony formation and suggest that miR-128 may exert tumor suppressive function in lung cancer cells by regulating PFKL-mediated cell growth.

MiR-128 expression is inversely correlated with PFKL mRNA level in lung cancer patients

To confirm the role of the miR-128-*PFKL* axis in human lung cancer patients, we examined *PFKL* mRNA level and miR-128 expression by qRT-PCR in 20 matched lung cancer samples and adjacent non-cancerous tissues. Importantly, levels of *PFKL* mRNA were shown to be significantly higher in lung cancer tissues compared to non-cancerous samples (**Figure 5A**), while levels of miR-128 were lower in lung cancer samples compared to non-cancerous tissues (**Figure 5B**). Using Pearson's correlation analysis, we determined that miR-128 expression was inversely correlated with *PFKL* mRNA levels (**Figure 5C**). Moreover, patients with higher *PFKL* expression were shown to exhibit poor overall survival (**Figure 5D**). Together, these results strongly indicate that high-expression of *PFKL* is significantly correlated with down-regulation of miR-128 and predicts lower survival in lung cancer patients.

MiR-128 regulates PFKL through AKT phosphorylation

Given that AKT signaling is known to stimulate a glycolytic switch in cancer cells [21, 22], we asked whether miR-128 regulates glycolysis via phosphorylation of AKT. Using western blot

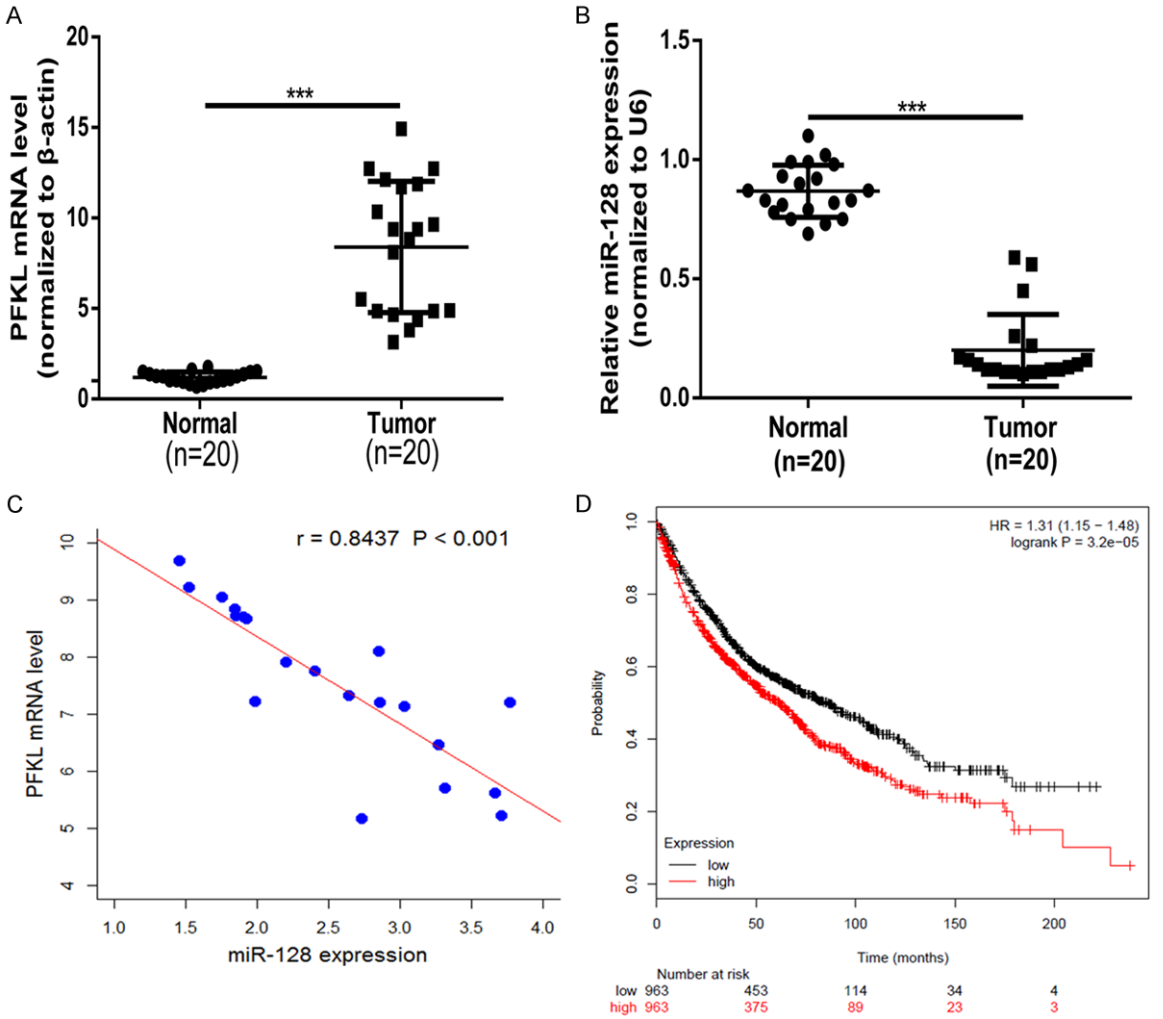

Figure 5. *PFKL* and miR-128 expression correlate in clinical samples. A, B. *PFKL* mRNA level and relative miR-128 expression were analyzed in cancer samples compared normal samples. C. The correlation between *PFKL* mRNA level and miR-128 expression was calculated in cancer samples. Data were subjected to Pearson correlation analysis. D. Kaplan-Meier analysis of the correlation between *PFKL* expression and overall survival of 1926 lung cancer patients. The symbol * denotes statistically significant differences with ***p < 0.001.

analysis, we showed that overexpression of miR-128 inhibited AKT phosphorylation, but not total AKT levels in lung cancer cells (**Figure 6A**). Interestingly, suppression of miR-128 had no detectable effect on levels of phosphorylated or total AKT protein (**Figure 6A**). Next, we determined whether negative feedback signaling from AKT effects miR-128 and *PFKL* expression by treating cells with the specific AKT inhibitor GSK690693. As shown in **Figure 6B**, **6C**, inhibition of AKT phosphorylation in NCI-H460 cells led to an increase in miR-128 expression and decrease in *PFKL* mRNA levels. Conversely, dysregulation of both miR-128 and *PFKL* had no effect on *AKT* expression at the mRNA level (Figure S3). Collectively, these results highlight a feedback loop between miR-128 and AKT signaling, and suggest that miR-128 may regulate glycolysis by targeting *PFKL* 3'UTR and inhibiting AKT phosphorylation in lung cancer (**Figure 6D**).

Discussion

It is well established that cancer cells largely depend on glycolysis to meet their energy demands, however, the molecular mechanism that drive metabolic shifts in caner cells are poorly understood. Here, we present data demonstrating that miR-128 plays a pivotal role in

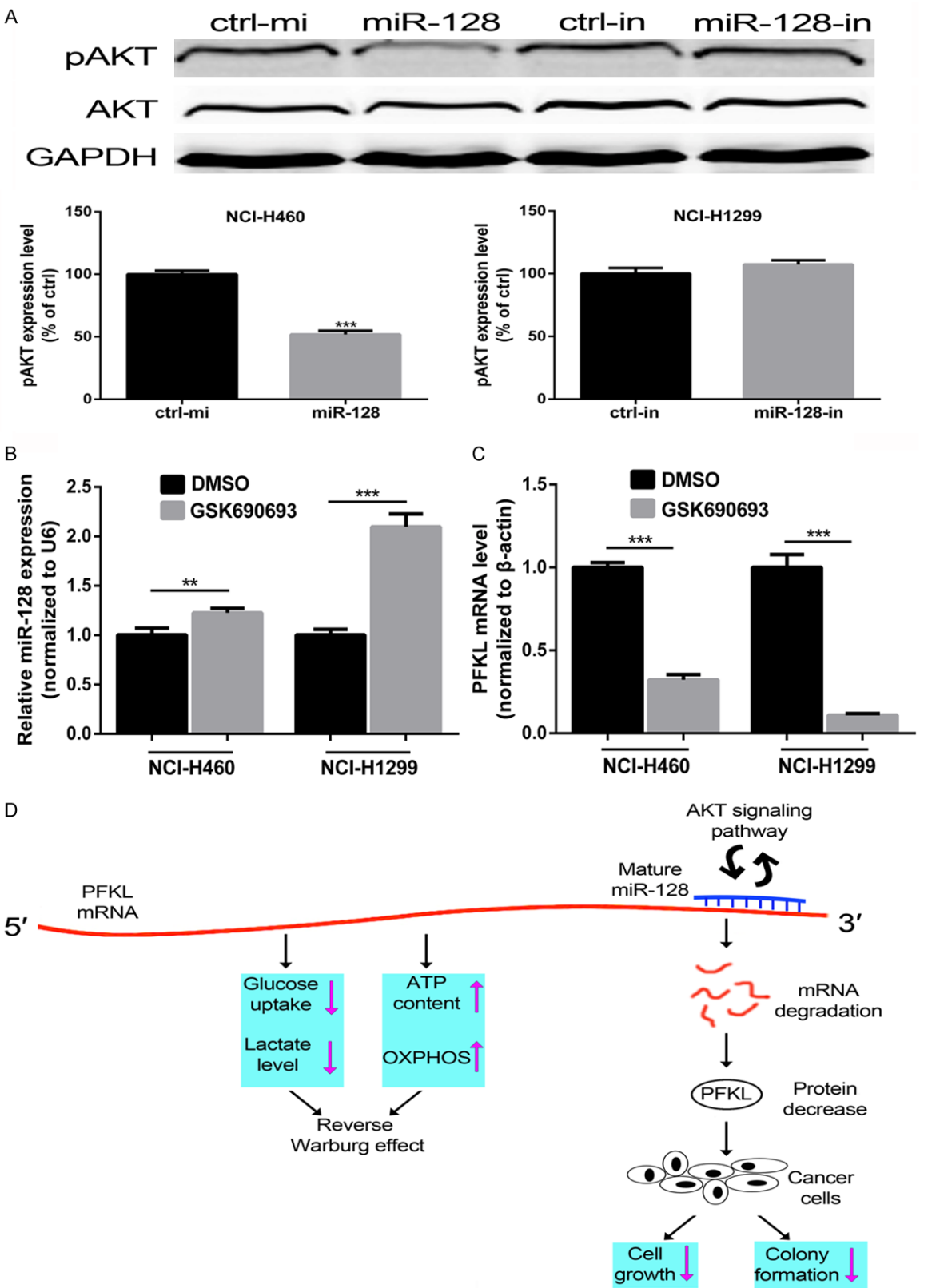

Figure 6. The AKT pathway is involved in miR-128 expression. A. Overexpression of miR-128 decreases AKT phosphorylation, but not total AKT protein levels. However, inhibition of miR-128 does not affect phosphorylated or total AKT protein levels. B. The AKT inhibitor, GSK690693, promotes expression of miR-128 as measured by qRT-PCR. C. GSK690693 suppresses the expression of *PFKL* as measured by qRT-PCR. D. Graphical representation of how

miR-128 regulates metabolic pathways to drive the Warburg effect in cancer cells. The symbol * shows statistically significant differences with **p < 0.01 and ***p < 0.001.

lung cancer cell glycolysis. In particular, we showed that miR-128 mediates a metabolic shift from glycolysis to OXPHOS by targeting *PFKL* and inhibiting AKT phosphorylation in lung cancer cells. Additionally, both miR-128 knockdown and *PFKL* overexpression promote lung cancer cell growth, colony formation, and decrease cellular ATP content. These findings suggest that miR-128 plays an essential role in regulating cancer cell glucose metabolism, cell growth and proliferation.

In an effort to limit cancer progression, attempts have been made over the past decade to therapeutically target glucose metabolism [23]. The Lin28/let-7 axis is a highly conserved pathway across mammals that can regulate diverse progression including cell fate and metabolism [24]. A recent study illustrates that the Lin28/let-7 axis regulates cancer progression and aerobic glycolysis via 3'-phosphoinositide-dependent kinase 1 (PDK1) in Hep3B cells [25]. In addition to its role in hepatocellular carcinoma cells, PDK1 has also been shown to regulate metabolic transition in glioblastoma multiforme. RNA-mediated attenuation of PDK1 and epidermal growth factor receptor (EGFR) has been shown to shift cellular metabolism from Warburg effect to OXPHOS, and subsequently suppress glioblastoma multiforme cell growth and proliferation [26]. These results show that targeting key enzymes (or components) that are involved in the Warburg effect may represent a useful strategy for cancer therapy.

Over the past decade, many studies have focused on non-coding RNAs (ncRNAs) that have been implicated in the Warburg effect. A recent study has suggested that miR-122, which is secreted by cancer cells, regulates glucose metabolism by downregulating pyruvate kinase, inhibiting glucose uptake in neighboring normal cells and reprogramming glucose consumption to adapt to cancer progression in the premetastatic microenvironment [27]. Long non-coding RNAs (lncRNAs) have also been reported to participate in cancer cell glycolysis. *PCGEM1* is a prostate-specific lncRNA that is induced by androgen and has been found overexpressed in prostate cancer [28]. *PCGEM1* promotes glycolysis by regulating the expression of enzymes that are involved in multiple glucose metabolic processes. As an additional mechanism, *PCGEM1* controls glucose metabolism via transcriptional regulation, specifically by binding to oncogenic c-Myc, which is a critical effector of *PCGEM1* [29]. Together, these studies demonstrate that targeting ncRNAs that regulate glucose metabolism may provide an effective therapeutic method to inhibit cancer progression.

In the present study, we show that miR-128 regulates *PFKL* in lung cancer cells by targeting one of three key metabolic enzymes and inhibiting AKT phosphorylation. We describe a novel miR-128-PFKL-AKT axis in lung cancer cells that mediates a switch in glucose consumption, lactate production and ATP generation, and drives cell proliferation and anchorage-independent growth. We show that miR-128 is inversely correlated with *PFKL* mRNA in lung cancer tissues and that high-expression of *PFKL*, induced by miR-128 downregulation, predicts poor overall patient survival. These findings suggest that miR-128 may act as tumor suppressor in lung cancer by regulating cancer cell glycolysis. Collectively, the multiple effects of miR-128 on the cancer cells demonstrate that miR-128 could be a powerful target for anti-cancer therapy.

Acknowledgements

We thank Dr. Dazhi Xu (State Key Laboratory of Oncology in South China) and Dr. Hui-Kuan Lin (The University of Texas MD Anderson Cancer Center) for constructive comments. This work was supported in part by research grants from the Natural Science Foundation of Zhejiang Province (LY15C060003 to Z. Gong), the Academic Climbing Project of Zhejiang Provincial Universities Discipline Leaders (pd-2013103 to Z. Gong), the Public Technology Applied Research Program of Zhejiang Province (2013C37029 to Y. Le), the Natural Science Foundation of Ningbo City (2015A610220 to Z. Gong), the Sci-Tech Project of Ningbo City (2014C50058 to Z. Gong) and the K.C.Wong Magna Fund at Ningbo University.

Disclosure of conflict of interest

None.

Address correspondence to: Zhaohui Gong, Department of Biochemistry and Molecular Biology, Ningbo University School of Medicine, 818 Fenghua Road, Ningbo 315211, ZJ, China. Tel: +86 574 87600740; Fax: +86 574 87608638; E-mail: zhaohui@ncri.org.cn

References

[1] WARBURG O. On respiratory impairment in cancer cells. Science 1956; 124: 269-270.

[2] WARBURG O. On the origin of cancer cells. Science 1956; 123: 309-314.

[3] Hatziapostolou M, Polytarchou C and Iliopoulos D. miRNAs link metabolic reprogramming to oncogenesis. Trends Endocrinol Metab 2013; 24: 361-373.

[4] Gyorffy B, Surowiak P, Budczies J and Lanczky A. Online survival analysis software to assess the prognostic value of biomarkers using transcriptomic data in non-small-cell lung cancer. PLoS One 2013; 8: e82241.

[5] Fantin VR, St-Pierre J and Leder P. Attenuation of LDH-A expression uncovers a link between glycolysis, mitochondrial physiology, and tumor maintenance. Cancer Cell 2006; 9: 425-434.

[6] Wang L, Xiong H, Wu F, Zhang Y, Wang J, Zhao L, Guo X, Chang LJ, Zhang Y, You MJ, Koochekpour S, Saleem M, Huang H, Lu J and Deng Y. Hexokinase 2-mediated Warburg effect is required for PTEN- and p53-deficiency-driven prostate cancer growth. Cell Rep 2014; 8: 1461-1474.

[7] Wegener G and Krause U. Different modes of activating phosphofructokinase, a key regulatory enzyme of glycolysis, in working vertebrate muscle. Biochem Soc Trans 2002; 30: 264-270.

[8] Yi W, Clark PM, Mason DE, Keenan MC, Hill C, Goddard WA 3rd, Peters EC, Driggers EM and Hsieh-Wilson LC. Phosphofructokinase 1 glycosylation regulates cell growth and metabolism. Science 2012; 337: 975-980.

[9] Moon JS, Jin WJ, Kwak JH, Kim HJ, Yun MJ, Kim JW, Park SW and Kim KS. Androgen stimulates glycolysis for de novo lipid synthesis by increasing the activities of hexokinase 2 and 6-phosphofructo-2-kinase/fructose-2,6-bisphosphatase 2 in prostate cancer cells. Biochem J 2011; 433: 225-233.

[10] Calin GA, Dumitru CD, Shimizu M, Bichi R, Zupo S, Noch E, Aldler H, Rattan S, Keating M, Rai K, Rassenti L, Kipps T, Negrini M, Bullrich F and Croce CM. Frequent deletions and down-regulation of micro- RNA genes miR15 and miR16 at 13q14 in chronic lymphocytic leukemia. Proc Natl Acad Sci U S A 2002; 99: 15524-15529.

[11] Kumar MS, Lu J, Mercer KL, Golub TR and Jacks T. Impaired microRNA processing enhances cellular transformation and tumorigenesis. Nat Genet 2007; 39: 673-677.

[12] Ding L, Xu Y, Zhang W, Deng Y, Si M, Du Y, Yao H, Liu X, Ke Y, Si J and Zhou T. MiR-375 frequently downregulated in gastric cancer inhibits cell proliferation by targeting JAK2. Cell Res 2010; 20: 784-793.

[13] Eichner LJ, Perry MC, Dufour CR, Bertos N, Park M, St-Pierre J and Giguere V. miR-378(*) mediates metabolic shift in breast cancer cells via the PGC-1beta/ERRgamma transcriptional pathway. Cell Metab 2010; 12: 352-361.

[14] Iorio MV and Croce CM. microRNA involvement in human cancer. Carcinogenesis 2012; 33: 1126-1133.

[15] Zhong Z, Dong Z, Yang L and Gong Z. miR-21 induces cell cycle at S phase and modulates cell proliferation by down-regulating hMSH2 in lung cancer. J Cancer Res Clin Oncol 2012; 138: 1781-1788.

[16] Dong Z, Zhong Z, Yang L, Wang S and Gong Z. MicroRNA-31 inhibits cisplatin-induced apoptosis in non-small cell lung cancer cells by regulating the drug transporter ABCB9. Cancer Lett 2014; 343: 249-257.

[17] Yang L, Yang J, Li J, Shen X, Le Y, Zhou C, Wang S, Zhang S, Xu D and Gong Z. MircoRNA-33a inhibits epithelial-to-mesenchymal transition and metastasis and could be a prognostic marker in non-small cell lung cancer. Sci Rep 2015; 5: 13677.

[18] Kent OA, McCall MN, Cornish TC and Halushka MK. Lessons from miR-143/145: the importance of cell-type localization of miRNAs. Nucleic Acids Res 2014; 42: 7528-7538.

[19] Fang R, Xiao T, Fang Z, Sun Y, Li F, Gao Y, Feng Y, Li L, Wang Y, Liu X, Chen H, Liu XY and Ji H. MicroRNA-143 (miR-143) regulates cancer glycolysis via targeting hexokinase 2 gene. J Biol Chem 2012; 287: 23227-23235.

[20] Jiang S, Zhang LF, Zhang HW, Hu S, Lu MH, Liang S, Li B, Li Y, Li D, Wang ED and Liu MF. A novel miR-155/miR-143 cascade controls glycolysis by regulating hexokinase 2 in breast cancer cells. EMBO J 2012; 31: 1985-1998.

[21] Elstrom RL, Bauer DE, Buzzai M, Karnauskas R, Harris MH, Plas DR, Zhuang H, Cinalli RM, Alavi A, Rudin CM and Thompson CB. Akt stimulates aerobic glycolysis in cancer cells. Cancer Res 2004; 64: 3892-3899.

[22] Manning BD and Cantley LC. AKT/PKB signaling: navigating downstream. Cell 2007; 129: 1261-1274.

[23] Nakano I. Therapeutic potential of targeting glucose metabolism in glioma stem cells. Expert Opin Ther Targets 2014; 18: 1233-1236.
[24] Thornton JE and Gregory RI. How does Lin28 let-7 control development and disease? Trends Cell Biol 2012; 22: 474-482.
[25] Ma X, Li C, Sun L, Huang D, Li T, He X, Wu G, Yang Z, Zhong X, Song L, Gao P and Zhang H. Lin28/let-7 axis regulates aerobic glycolysis and cancer progression via PDK1. Nat Commun 2014; 5: 5212.
[26] Velpula KK, Bhasin A, Asuthkar S and Tsung AJ. Combined targeting of PDK1 and EGFR triggers regression of glioblastoma by reversing the Warburg effect. Cancer Res 2013; 73: 7277-7289.
[27] Fong MY, Zhou W, Liu L, Alontaga AY, Chandra M, Ashby J, Chow A, O'Connor ST, Li S, Chin AR, Somlo G, Palomares M, Li Z, Tremblay JR, Tsuyada A, Sun G, Reid MA, Wu X, Swiderski P, Ren X, Shi Y, Kong M, Zhong W, Chen Y and Wang SE. Breast-cancer-secreted miR-122 reprograms glucose metabolism in premetastatic niche to promote metastasis. Nat Cell Biol 2015; 17: 183-194.
[28] Srikantan V, Zou Z, Petrovics G, Xu L, Augustus M, Davis L, Livezey JR, Connell T, Sesterhenn IA, Yoshino K, Buzard GS, Mostofi FK, McLeod DG, Moul JW and Srivastava S. PCGEM1, a prostate-specific gene, is overexpressed in prostate cancer. Proc Natl Acad Sci U S A 2000; 97: 12216-12221.
[29] Hung CL, Wang LY, Yu YL, Chen HW, Srivastava S, Petrovics G and Kung HJ. A long noncoding RNA connects c-Myc to tumor metabolism. Proc Natl Acad Sci U S A 2014; 111: 18697-18702.

Table S1. Sequences of RNAi used for cell transfection

Name	Sequence
ctrl-mimics	Sense: 5'-UUC UCC GAA CGU GUC ACG UTT-3'
	Anti-sense: 5'-ACG UGA CAC GUU CGG AGA ATT-3'
has-miR-128 mimics	Sense: 5'-UCA CAG UGA ACC GGU CUC UUU-3'
	Anti-sense: 5'-AGA GAC CGG UUC ACU GUG AUU-3'
ctrl-inhibitor	5'-CAG UAC UUU UGU GUA GUA CAA-3'
has-miR-128 inhibitor	5'-AAA GAG ACC GGU UCA CUG UGA-3'
ctrl-siRNA	Sense: 5'-UUC UCC GAA CGU GUC ACG UTT-3'
	Anti-sense: 5'-ACG UGA CAC GUU CGG AGA ATT-3'
PFKL-siRNA	Sense: 5'-GCA UCG UCA UGU GUG UCA UTT-3'
	Anti-sense: 5'-AUG ACA CAC AUG ACG AUG CTT-3'
AKT-siRNA	Sense: 5'-GAC GGG CAC AUU AAG AUC ATT-3'
	Anti-sense: 5'-UGA UCU UAA UGU GCC CGU CTT-3'

Table S2. Primer sequences used for PCR and qRT-PCR and general-PCR

Name/Primer	Forward primer	Reverse primer
PFKL	CATCAGCAACAACGTCCCTG	GGCCAGGTAGCCACAGTAAC
AKT	CACTTTCGGCAAGGTGATCC	ATGACAAAGCAGAGGCGGTC
β-actin	ACAGGCATCGTGATGGATTCT	CAGCAGTGGTGGTGAAGTTAT
PFKL 3'UTR-WT	TCAGCAGTCGAAGAGCCCTGG GCTGTTGTGTCTGGA	TTAGCGTGTGAAGAGCTCAC AGTGAGGCAGGGCCA
PFKL 3'UTR-Mut	TCAGCAGTCGAAGAGCCCTG GGCTGTTGTGTCTGGA	TTAGCGTGTGAAGAGCTAGG CAGGGCCAGGGGCA
PFKL-ORF	TCAGCAGTCGAAGAGCATGA GAAGCATGTGTAACCA	TTAGCGTGTGAAGAGCTCAG AAGCCCTTGTCCATGC

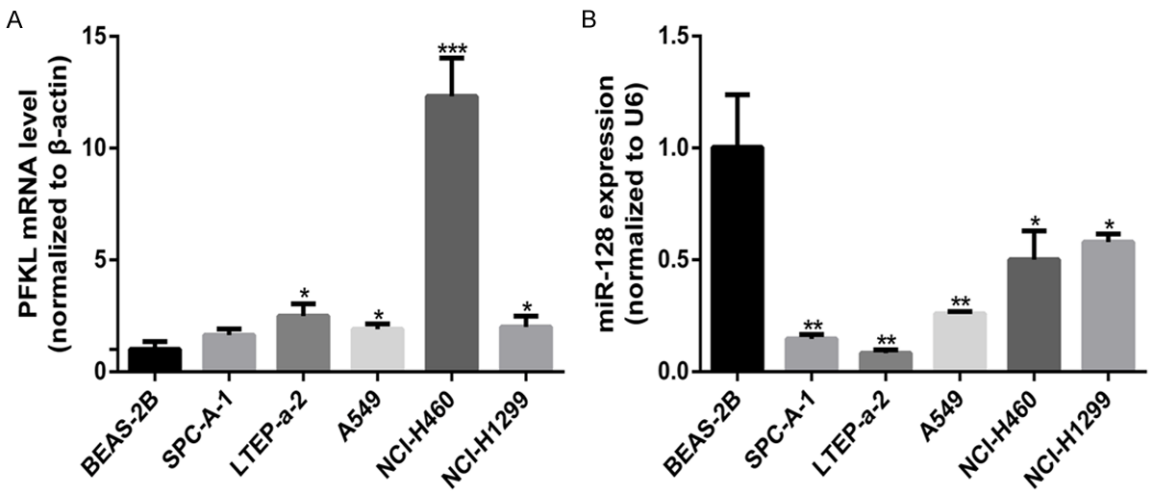

Figure S1. miR-128 is lowly expressed in lung cancer cells. A. Basal expression of miR-128 in BEAS-2B and five lung cancer cells. B. Basal *PFKL* expression in BEAS-2B and five lung cancer cells. Results are presented as mean ± SEM, n = 3. Student t test was used for evaluation of statistical significance in A, B. The symbol * shows statistically significant differences with *$p < 0.05$, **$p < 0.01$ and ***$p < 0.001$.

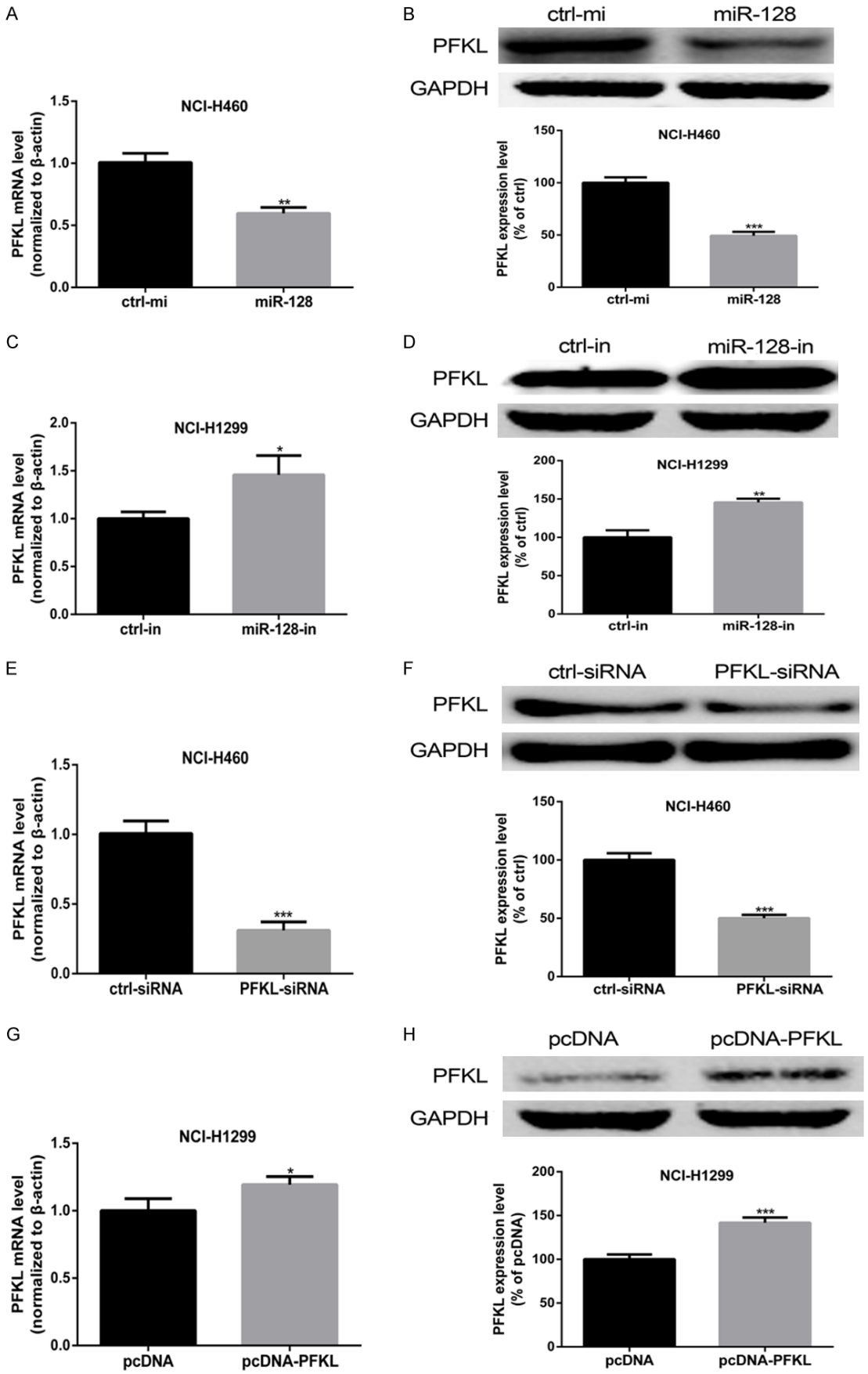
A
NCI-H460
PFKL mRNA level (normalized to β-actin)
1.5
1.0
0.5
0.0
**
ctrl-mi
miR-128
B
ctrl-mi
miR-128
PFKL
GAPDH
NCI-H460
PFKL expression level (% of ctrl)
150
100
50
0
***
ctrl-mi
miR-128
C
NCI-H1299
PFKL mRNA level (normalized to β-actin)
2.0
1.5
1.0
0.5
0.0
*
ctrl-in
miR-128-in
D
ctrl-in
miR-128-in
PFKL
GAPDH
NCI-H1299
PFKL expression level (% of ctrl)
200
150
100
50
0
**
ctrl-in
miR-128-in
E
NCI-H460
PFKL mRNA level (normalized to β-actin)
1.5
1.0
0.5
0.0
***
ctrl-siRNA
PFKL-siRNA
F
ctrl-siRNA
PFKL-siRNA
PFKL
GAPDH
NCI-H460
PFKL expression level (% of ctrl)
150
100
50
0
***
ctrl-siRNA
PFKL-siRNA
G
NCI-H1299
PFKL mRNA level (normalized to β-actin)
1.5
1.0
0.5
0.0
*
pcDNA
pcDNA-PFKL
H
pcDNA
pcDNA-PFKL
PFKL
GAPDH
NCI-H1299
PFKL expression level (% of pcDNA)
200
150
100
50
0
***
pcDNA
pcDNA-PFKL

Figure S2. miR-128 regulates *PFKL* at mRNA and protein levels. A-D. H460 and H1299 cells were transfected with miR-128 and miR-128-in, respectively. The level of *PFKL* was measured by qRT-PCR and Western blot. E-H. H460 and H1299 cells were transfected with *PFKL* siRNA and pcDNA-PFKL, respectively. The level of *PFKL* was measured by qRT-PCR and Western blot. Results are presented as mean ± SEM, n = 3. Student t test was used for evaluation of statistical significance in A-H.The symbol * indicates statistically significant differences with *p < 0.05, **p < 0.01 and ***p < 0.001.

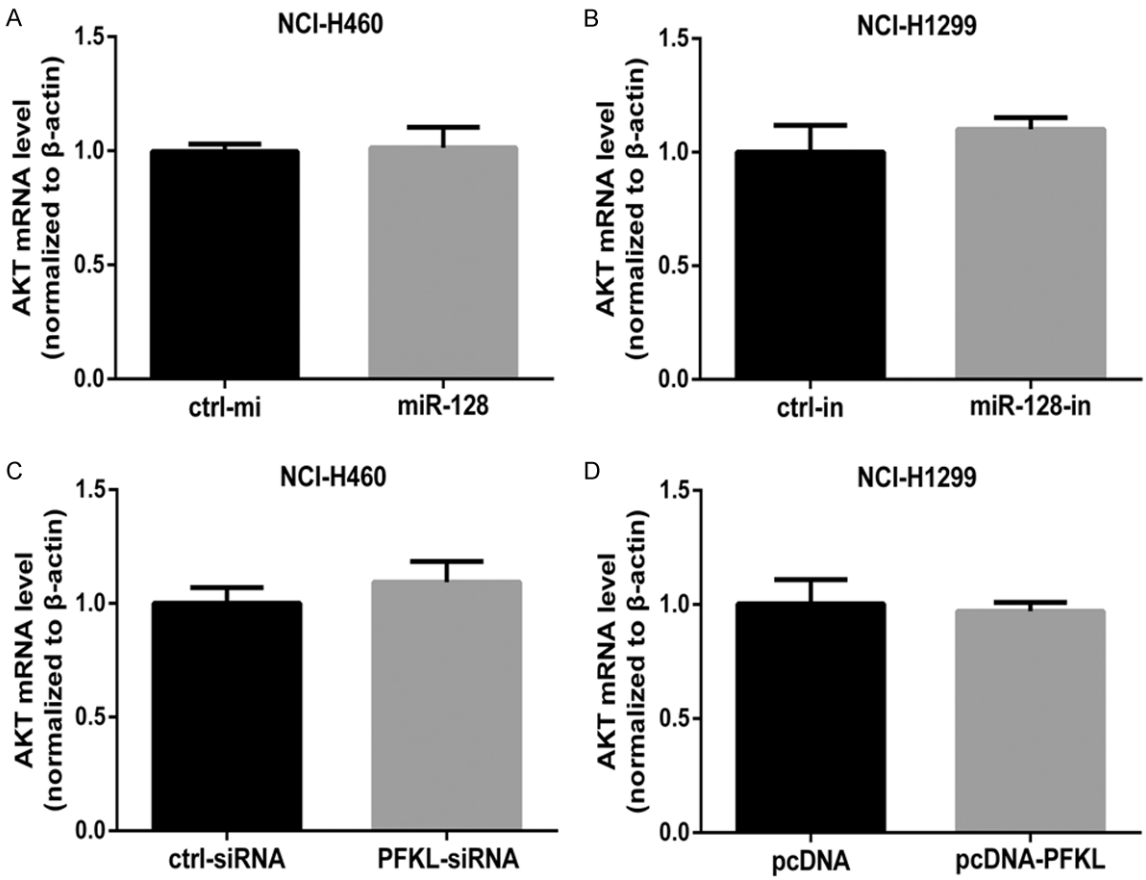

Figure S3. miR-128 has no significant effect on *AKT* mRNA level. A and B. H460 and H1299 cells were transfected with miR-128 and miR-128-in, respectively. The mRNA level of *AKT* was confirmed by qRT-PCR. C and D. H460 and H1299 cells were transfected with *PFKL* siRNA and pcDNA-PFKL, respectively. And then qRT-PCR was used to measure the expression of *AKT* mRNA level. Data are from three independent experiments and results are represented as mean ± SEM. Student t test was used for evaluation of statistical significance in A-D.